

A Novel Cyber-Physical System For The Optimal Heating-Cooling of Buildings

Mahdiyar Barzegar and Alireza Farhadi

Abstract—This paper presents a novel Cyber-Physical System (CPS) equipped with an advanced Distributed Model Predictive Control (DMPC) method with reduced order computational complexity, zero steady-state error, reduced start-up energy consumption and improved transient response for the optimal heating-cooling of buildings. The satisfactory application of this method for the optimal heating-cooling of a large-scale (6-story) building with 40 rooms is illustrated. Smart Industrial Internet of Things (IIoT) - based thermostats, a gateway and a general Quadratic Programming (QP) solver are developed. Using this hardware set-up, the simulation results for the 6-story building are verified in a small scale by practical implementation.

Note to Practitioners—This paper proposes a novel cyber-physical system for the optimal heating-cooling of large-scale buildings. The proposed system is practical, in particular, for large-scale buildings because for its realization, we do not need mighty and therefore expensive computer servers to execute required optimization problems in real-time. It also has high reliability and resilience due to its distributed computation nature and can be realized using available and cost-effective On-Off electric valves. To implement this system, a general QP solver, smart IIoT-based thermostats and a gateway are designed, developed and implemented in a building for the optimal heating and cooling. The satisfactory performance and superiority of the proposed system in terms of zero steady-state error, transient response, applicability for both heating and cooling systems and limited start-up energy consumption over the traditional as well as more advanced systems are illustrated by simulation and practical implementation.

Index Terms—Distributed model predictive control, cyber-physical system, building automation and control.

I. INTRODUCTION

A. Motivation and Backgrounds

ONE of the growing applications of the Industrial Internet of Things (IIoT) is in the building automation and control systems. More than 40 percent of the world's energy consumption is related to the heating-cooling of buildings. In contrast, the performance of the commonly used traditional hysteresis-based control method for the heating-cooling of buildings is low. The structure of the multi-zone temperature control system for buildings is depicted in Fig.1. Due to its structure, the Model Predictive Control (MPC) is a suitable method for designing a MIMO controller based on an integrated large-scale thermal dynamic model of building for the optimal heating and cooling [1]. This MPC controller can be realized as centralized, decentralized, or distributed.

One of the commonly used control structures is the centralized structure. The centralized structure gets all the system's information, then calculates the control law of all the inputs together, and sends the control signals to the actuators via the network. The control structure could achieve the best dynamic performance of the closed-loop system. However, since there are hundreds (or thousands) of input and output variables in a large-scale system, the computational burden is unavoidably high if all control variables are solved together by a centralized controller hosted in a centralized computer. To understand this computational complexity drawback, note that the computational complexity associated with the centralized constrained optimization problem can be of the order of $O(n^5)$ [2]. Thus, for a large-scale system with thousands of control inputs, it takes lots of time to calculate the control law of all the inputs; while this calculation should be done almost instantaneously. To overcome this drawback, the decentralized control structure has been proposed in the literature [1]. In the decentralized control structure, we decompose the centralized controller into many relevant small scaled controllers. These controllers work independently even when the corresponding controlled subsystems are coupled with each other. These controllers have the advantages of simple structure, less computational burden, better error tolerance, good flexibility, and accessible design and implementation. However, since there is no communication and coordination among decentralized controllers, the controller performance is destroyed if the coupling among subsystems is strong enough. The traditional hysteresis - based control method for the heating-cooling of buildings [3] is an example of a control system with a fully decentralized structure. To overcome the performance degradation drawback of the decentralized control structure and at the same time have the advantages of the decentralized controller, the distributed control structure has been proposed [1], [4], [5], [6]. In this control structure, the computational load of the centralized controller is distributed to distributed computational units. This paper is concerned with this control structure with application in the optimal heating-cooling of buildings.

In [7], a Jacobi interactive-based algorithm that distributes the computational load of the convex optimization problem with quadratic cost function to distributed optimizers has been proposed; and its application in automated irrigation networks has been illustrated. In [4], a DMPC method for the optimal heating-cooling of buildings was presented. In the proposed method in [4], the start-up energy consumption of the HVAC system may be high; because it only includes constraints on HVAC units temperature; and it does not consider constraints

This paper was produced by the IEEE Publication Technology Group. They are in Piscataway, NJ.

Manuscript received X X, X; revised X X, X.

This work was supported by Iran's National Elites Foundation.

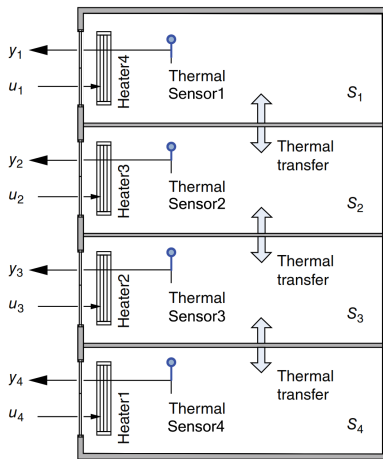


Fig. 1: The multi-zone building temperature control system [1]

on the rate, which HVAC units temperature, changes. Also, in [4] there is a trade-off between steady-state error and the optimal set-points for HVAC units; and hence, there is always a steady-state error between rooms temperature and the desired set points. It also presents an optimization problem that is only suitable for the heating system and it does not use the weather forecast to improve the transient response of the system. [5], [8] and [9] suffer from the same drawbacks. [10] and [11] propose centralized MPC for the optimal heating of buildings; and hence, they are not suitable for large-scale buildings. They also suffer from non-zero steady state error and do not include the weather forecast to improve the transient response. They may also suffer from high start-up energy consumption. [12] and [13] use the weather forecast in their formulation; but they suffer from high start-up energy consumption, non-zero steady state error and a problem formulation that is only suitable for the heating system. In [14], an advanced optimal On-Off control method for temperature control in a decentralized structure has been proposed. Decentralized structure for the proposed control method of [14] may decrease the performance of the whole HVAC building system; because the thermal exchange between sub-systems are not considered. Also, the proposed structure in [14] does not implement feed forward strategy to compensate measurable disturbances, such as outside temperature. In [15], the application of MPC in the optimal heating-cooling of buildings in three different structures: centralized, decentralized, and distributed has been presented. The cost function used in the MPC method of [15] has four terms that could impose a large computational load on the system and need expensive computer server and processors to guarantee real-time computation and decision making for large-scale buildings. In addition, it may suffer from non-zero steady-state error and high start-up energy consumption. [16], [17] use a centralized MPC algorithm for the optimal heating of building; and hence, the proposed structure is not suitable for large-scale buildings. They also suffer from non-zero steady state error and high start-up energy consumption. [18] proposes a method for controlling a room temperature using both the fan speed and temperature of fan-coil unit. It uses a non-linear dynamic model and a decentralized MPC

algorithm. [19] also presents a decentralized MPC algorithm for the temperature regulation of a room with zero steady state error. It also uses the weather forecast for the temperature regulation. [18] and [19] use decentralized structure and hence they do not consider the thermal interaction between sub-systems. Thus, generally speaking, their performance is not as good as centralized or distributed structures considered in this paper. [20] presents an application of IIoT for the optimal heating-cooling of buildings. It uses weather forecast to reduce the energy consumption for heating and cooling. However, the proposed HVAC system suffers from large steady - state error. [21] proposes a centralized MPC algorithm for the optimal temperature regulation of building that uses the weather forecast. [22] presents a centralized MPC algorithm equipped with a filter for the estimation of the thermal parameters of building. It suffers from non-zero steady state error and high start up energy consumption. [21] and [22] use centralized structure and hence they are not suitable for large-scale buildings. [23], [24], [25] also use centralized structure. [23] and [24] suffer from non-zero steady-state error and it does not use weather forecast. Also, [25] does not use weather forecast. [26] is a survey paper of MPC algorithms developed for the optimal temperature regulation. We reviewed some of the most important MPC algorithms presented in [26] in the above literature review.

B. Paper Contributions

Our extensive literature review reveals that most of the available controllers for HVAC system in the literature are either centralized and therefore are not suitable for large-scale buildings; or decentralized and therefore have poor performance. This said, this paper aims to fill the gap in the literature by proposing a novel distributed control method with reduced computational complexity that is particularly suitable for implementation in large – scale buildings. Comparing to other available distributed control methods for HVAC system, the proposed method has simple cost function, its formulation is suitable for both seasons and it results in zero steady-state error, with reduced start-up energy consumption and improved transient response. Specifically, in this paper, we propose the Embedded Integrator (EI)-MPC method by embedding an integrator in the dynamic system. In the proposed method we use the weather forecast to improve the transient response. In fact, this paper proposes a novel IIoT system for the optimal heating-cooling of buildings that is equipped with the above distributed EI-MPC. In this system, the computational load of the centralized MPC controller is distributed to smart IIoT-based thermostats that are distributed in building. Geographically separated smart thermostats collaborate and communicate with each other in wireless to generate proper control inputs in real time with reduced order computational complexity. In the proposed IIoT system, the computation (cyber) resource is integrated with the physical world forming a new type of IIoT system known as Cyber-Physical System (CPS). In the proposed CPS the computational load is distributed in the field layer (i.e., distributed smart thermostats); and therefore, we do not need a powerful centralized computer server to carry

out the required computation for the optimization. Hence, the proposed cyber-physical system is relatively cheaper than the ordinary IIoT systems. Scalability and much higher reliability, which are due to its distributed nature, are other advantages of the proposed system over the IIoT systems.

C. Paper Organization

The paper is organized as follows: the introduction was given in Section I. The EI-MPC problem is formulated for the optimal heating-cooling buildings in Section II followed by a short description of the Jacobi iterative-based algorithm that distributes the computation load of this method to distributed optimizers. The reduced order optimization problems to be solved by distributed optimizers is presented in Section III, followed by the QP solver. In Section IV, the structure of the proposed cyber-physical system is presented. The simulation results are presented in Section V; and the superiority of the proposed cyber-physical system in the optimal heating-cooling of buildings over the available DMPC-based methods and the traditional hysteresis-based method is presented. The simulation results presented in Section V are verified in a small-scale in Section VI via practical implementation by equipping one of the room of the 6-story building used for simulation with two smart IIoT - based thermostats and a gateway that we design and develop. The paper is finally concluded in Section VII.

II. EI-MPC

In this section, we first formulate the EI-MPC method, and then we briefly describe the Jacobi iterative method introduced in [7] that distributes the computational load of the EI-MPC to distributed optimizers.

A. EI-MPC Problem Formulation

Model predictive control is designed based on a mathematical model for the system. The model to be used in the control system design is the state space model. Utilizing the state space model, the current information required for the prediction is represented by the state variable at the current time. In general, to design the model predictive control, we use the state space model for a multi-input and multi-output system as follows:

$$\begin{aligned} x_m[k+1] &= A_m x_m[k] + B_m u[k] + E_m d[k] \\ y[k] &= C_m x_m[k] \end{aligned} \quad (1)$$

where x_m is the state variable with the size of n_s , u is the decision variable with the size of n_u , d is the measurable disturbance to the system with the size of n_d and y is the process output of the system with the size of n_o .

Now, we need to re-write the model to suit for our design purpose where an integrator is embedded. Taking a difference operation on both sides of (1), we obtain that $x_m[k+1] - x_m[k] = A_m(x_m[k] - x_m[k-1]) + B_m(u[k] - u[k-1]) + E_m(d[k] - d[k-1])$. Let us denote the difference of the state variable by $\Delta x_m[k+1] = x_m[k+1] - x_m[k]$ and $\Delta x_m[k] = x_m[k] - x_m[k-1]$, the difference of the control

variable by $\Delta u[k] = u[k] - u[k-1]$, and the difference of measurable disturbance by $\Delta d[k] = d[k] - d[k-1]$. These are the increments of the variables $x_m[k]$, $u[k]$, and $d[k]$, respectively. With this transformation, the difference state space equation is:

$$\Delta x_m[k+1] = A_m \Delta x_m[k] + B_m \Delta u[k] + E_m \Delta d[k] \quad (2)$$

Note that the input to the above state space model is $\Delta u[k]$. Now we connect $\Delta x_m[k]$ to the output $y[k]$. To do so, a new state variable vector is chosen to be $x[k] = \begin{bmatrix} \Delta x_m[k] \\ y[k] \end{bmatrix}$. Note that

$$\begin{aligned} y[k+1] - y[k] &= C_m(x_m[k+1] - x_m[k]) = C_m \Delta x_m[k+1] \\ &= C_m A_m \Delta x_m[k] + \\ &C_m B_m \Delta u[k] + C_m E_m \Delta d[k] \end{aligned} \quad (3)$$

Putting together (2) and (3) leads to the following state space model:

$$\begin{aligned} x[k+1] &= Ax[k] + B\Delta u[k] + E\Delta d[k] \\ y[k] &= Cx[k] \\ \begin{bmatrix} \Delta x_m[k+1] \\ y[k+1] \end{bmatrix} &= \begin{bmatrix} A_m & \mathbf{0}_1^{\text{tr}} \\ C_m A_m & \mathbf{1}_m \end{bmatrix} \begin{bmatrix} \Delta x_m[k] \\ y[k] \end{bmatrix} + \\ &\begin{bmatrix} B_m \\ C_m B_m \end{bmatrix} \Delta u[k] + \begin{bmatrix} E_m \\ C_m E_m \end{bmatrix} \Delta d[k] \\ y[k] &= [\mathbf{0}_2 \quad \mathbf{1}_m] \begin{bmatrix} \Delta x_m[k] \\ y[k] \end{bmatrix} \end{aligned} \quad (4)$$

where, the augmented model matrices (A, B, E, C) can be defined as:

$$\begin{aligned} A &= \begin{bmatrix} A_m & \mathbf{0}_1^{\text{tr}} \\ C_m A_m & \mathbf{1}_m \end{bmatrix}, B = \begin{bmatrix} B_m \\ C_m B_m \end{bmatrix}, E = \begin{bmatrix} E_m \\ C_m E_m \end{bmatrix}, \\ C &= [\mathbf{0}_2 \quad \mathbf{1}_m]. \end{aligned}$$

where $\mathbf{0}_1$ is a zero matrix with the size of n_s rows and n_o columns, $\mathbf{0}_2$ is a zero matrix with the size of n_o rows and n_s columns, $\mathbf{1}_m$ is an eye square matrix with the size of n_o . Upon formulation of this mathematical model, the next step in the design of a predictive control system is to calculate the predicted plant output with the future control signal as the adjustable variables. This prediction is described within an optimization window. Here, we assume that the current time is k_i and the length of the optimization window is N_p . Assuming that at the sampling instant $k_i > 0$, the state variable vector $x[k_i]$ is available through measurement, the state $x[k_i]$ provides the current plant information. The future control trajectory is denoted by: $\Delta U = [\Delta u[k_i]^{tr} \quad \Delta u[k_i+1]^{tr} \quad \dots \quad \Delta u[k_i+N_c-1]^{tr}]^{tr}$, where N_c is called the control horizon dictating the number of parameters used to capture the future control trajectory. The future measurable disturbance trajectory is denoted by: $\Delta D = [\Delta d[k_i]^{tr} \quad \Delta d[k_i+1]^{tr} \quad \dots \quad \Delta d[k_i+N_p-1]^{tr}]^{tr}$. With given information $x[k_i]$, the future state variables are predicted for N_p number of samples, where N_p is called the prediction horizon. N_p is also the length of the optimization window. We denote the future state variables as: $x[k_i+1|k_i], x[k_i+2|k_i], x[k_i+m|k_i], \dots, x[k_i+N_p|k_i]$,

where $x[k_i + m|k_i]$ is the predicted state variable at the time instant $k_i + m$ with the given current plant information $x[k_i]$. Subsequently, the predicted output is $y[k_i + m|k_i] = Cx[k_i + m|k_i]$ and the future output trajectory is $Y = [y[k_i + 1|k_i]^{tr} \ y[k_i + 2|k_i]^{tr} \ \dots \ y[k_i + N_p|k_i]^{tr}]^{tr}$. The control horizon N_c is chosen to be less than (or equal to) the prediction horizon N_p . Based on the state-space model (A, B, E, C) , the predicted output variables are calculated sequentially using the set of future control parameters:

$$y(k_i + m|k_i) = CA^m x(k_i) + \sum_{i=\max(0, m-N_c)}^{m-1} CA^i B \Delta u(k_i + m - 1 - i) + \sum_{i=0}^{m-1} CA^i E \Delta d(k_i + N_p - 1 - i) \quad m \in \{1, \dots, N_p\} \quad (5)$$

Note that all predicted variables are formulated in terms of the current state variable information $x[k_i]$ and the future control movement $\Delta u[k_i + j]$, where $j = 0, 1, \dots, N_c - 1$. We collect the above equations together in a compact matrix form as:

$$Y = Fx[k_i] + \Phi \Delta U + Z \Delta D,$$

$$F = \begin{bmatrix} CA \\ CA^2 \\ \vdots \\ CA^{N_p} \end{bmatrix}, \Phi = \begin{bmatrix} CB & 0 & \dots & 0 \\ CAB & CB & \dots & 0 \\ CA^2 B & CAB & \dots & 0 \\ \vdots & \vdots & \vdots & \vdots \\ CA^{N_p-1} B & CA^{N_p-2} B & \dots & CA^{N_p-N_c} B \end{bmatrix},$$

$$Z = \begin{bmatrix} CE & 0 & \dots & 0 \\ CAE & CE & \dots & 0 \\ CA^2 E & CAE & \dots & 0 \\ \vdots & \vdots & \vdots & \vdots \\ CA^{N_p-1} E & CA^{N_p-2} E & \dots & CA^{N_p-1} E \end{bmatrix}.$$

Denote the set-point signal vector by $r[k_i]$ at the sample time k_i , then the vector of the future desired set-points is:

$$R_s^{tr} = [r[k_i + 1]^{tr} \ r[k_i + 2]^{tr} \ \dots \ r[k_i + N_p]^{tr}].$$

Now, we can rewrite the cost function J that reflects the control objective as follows:

$$J = \|R_s - Y\|_Q + \|\Delta U\|_R \\ = (R_s - Y)^{tr} Q (R_s - Y) + \Delta U^{tr} R \Delta U,$$

where Q and R are the diagonal weighting matrices. To find the optimal ΔU that minimizes J , we express J as:

$$J = (R_s - Fx_k - Z \Delta D)^{tr} Q (R_s - Fx_k - Z \Delta D) \\ + 2(Fx_k + Z \Delta D - R_s)^{tr} (Q + Q^{tr})^{tr} \Phi \Delta U \\ + \Delta U^{tr} (\Phi^{tr} Q \Phi + R) \Delta U$$

Finally, we can define the optimization problem to be solved in order to find the optimal ΔU as the following standard convex quadratic optimization problem: $\min_{\Delta U} [\frac{1}{2} \Delta U^{tr} P \Delta U +$

$C^{tr} \Delta U]$ subject to

$$\Delta u_{min} \leq \Delta u[k_i + q] \leq \Delta u_{max}, \\ u_{min} - u[k_i + q - 1] \leq \Delta u[k_i + q] \leq u_{max} - u[k_i + q - 1], \\ u[k_i + q] = u[k_i - 1] + \sum_{j=0}^q \Delta u[k_i + j], \\ P = 2(\Phi^{tr} Q \Phi + R), \\ C = \Phi^{tr} (Q + Q^{tr}) (Fx[k_i] + Z \Delta D - R_s), \\ q \in \{0, 1, \dots, N_c - 1\}$$

After solving this optimization problem, $u[k_i]$ is applied to the system (1) and the above optimization problem is formulated and solved for the next time step $k_i + 1$.

B. The Jacobi based Iterative Algorithm

The Jacobi-based iterative algorithm proposed in [7] approximates the solution of the following convex optimization problem with the cost function of J (which is a quadratic function of the decision variables u_1, u_2, \dots, u_n) subject to the convex constraint sets \mathcal{U}_i .

$$\min_{u_i \in \mathcal{U}_i} J(u_1, u_2, \dots, u_n), \quad i = \{1, 2, \dots, n\}. \quad (6)$$

Note that the optimization problem formulated in the previous section is of the type of the above optimization problem; and therefore, the following algorithm can be used to approximate the solution of the optimization problem of the previous section with the computational complexity of $\mathcal{O}(n)$ [2]. Note that for large-scale buildings, the computational complexity of the Jacobi iterative algorithm is much less than the computational complexity of the conventional centralized methods (e.g., the active set method, the interior point method) that are of the order of $\mathcal{O}(n^5)$ [2]. Here, it is assumed that an optimizer exists for each decision variable; and optimizers form a connected communication graph so that each optimizer can communicate with all other optimizers. Having that, the Jacobi iterative algorithm consists of the following two steps:

Initialization: At the first iteration, i.e., $t = 0$, each optimizer chooses an arbitrary but feasible (i.e., $u_i^0 \in \mathcal{U}_i$) value for its decision variable. Then, it shares it with all other optimizers. Therefore, in the beginning, each optimizer knows the value of its decision variable and other optimizers decision variables. After initialization step, we have the second step, which is the update and all to all communication as follows:

Update and Communication: At the iteration $t \geq 1$, all of the optimizers in parallel update their decision variables as follows by focusing only on their decision variables and fixing the decision variables of other optimizers.

$$h_i^* = \operatorname{argmin}_{h_i \in \mathcal{U}_i} J(u_1^{t-1}, u_2^{t-1}, \dots, u_{i-1}^{t-1}, h_i, u_{i+1}^{t-1}, \dots) \\ u_i^t = \lambda_i h_i^* + (1 - \lambda_i) u_i^{t-1}. \quad (7)$$

where in the above relations, $\lambda_i \in \mathbb{R}$ are chosen a priori as follows: $0 < \lambda_i < 1$, $\sum_{i=1}^n \lambda_i = 1$. After each update, all optimizers share their updated decision variables u_i^t with other optimizers, and the above procedure is repeated for the next iteration $t + 1$. Note that since in the above two-step algorithm, each optimizer solves a reduced order optimization problem

by focusing on its decision variable in parallel with other optimizers at each update, the required time for finding the solution using this algorithm is relatively much smaller than that of the conventional centralized techniques, particularly for large scale problems. It is proved in [7] that the above iterative solution converges to the unique optimal solution of the convex optimization problem (6).

III. THE REDUCED ORDER OPTIMIZATION PROBLEM

The main objective of this paper is to distribute the computational load of the optimization problem of the previous section to distributed optimizers using the Jacobi iterative method. In other words, we need to decompose the above optimization problem with the number of $N_c \times n_u$ decision variables to n_u quadratic convex optimization problems with the number of N_c decision variables. In this section, we present this reduced-order optimization problem. Note that in the centralized optimization problem of previous section if we choose ΔU as follows: $\Delta U^{tr} = [\Delta u_1[k_i+1]^{tr} \ \Delta u_2[k_i+1]^{tr} \ \dots \ \Delta u_{n_u}[k_i+1]^{tr} \ \Delta u_1[k_i+2]^{tr} \ \Delta u_2[k_i+2]^{tr} \ \dots \ \Delta u_{n_u}[k_i+2]^{tr} \ \dots \ \Delta u_1[k_i+N_c]^{tr} \ \Delta u_2[k_i+N_c]^{tr} \ \dots \ \Delta u_{n_u}[k_i+N_c]^{tr}]$, then the reduced order optimization problem to be solved by the $\rho \in \{1, 2, \dots, n_u\}$ optimizer is described as follows:

$$\begin{aligned} & \min_{\Delta U_\rho} \left[\frac{1}{2} \Delta U_\rho^{tr} H_\rho \Delta U_\rho + G_\rho^{tr} \Delta U_\rho \right] \\ & \text{subject to} \\ & \Delta u_{min} \leq \Delta u_\rho[k_i+q] \leq \Delta u_{max}, \\ & u_{min} - u_\rho[k_i+q-1] \leq \Delta u_\rho[k_i+q] \leq u_{max} - u_\rho[k_i+q-1], \\ & u_\rho[k_i+q] = u_\rho[k_i-1] + \sum_{j=0}^q \Delta u_\rho[k_i+j], \\ & q \in \{0, 1, \dots, N_c-1\}, \\ & \Delta U_\rho = \begin{bmatrix} \Delta u_\rho[k_i+1] \\ \Delta u_\rho[k_i+2] \\ \vdots \\ \Delta u_\rho[k_i+N_c] \end{bmatrix}, \\ & H_\rho = \begin{bmatrix} h_{1,1\rho} & h_{1,2\rho} & \dots & h_{1,N_c\rho} \\ h_{2,1\rho} & h_{2,2\rho} & \dots & h_{2,N_c\rho} \\ \vdots & \vdots & \ddots & \vdots \\ h_{N_c,1\rho} & h_{N_c,2\rho} & \dots & h_{N_c,N_c\rho} \end{bmatrix}, G_\rho = \begin{bmatrix} g_{1\rho} \\ g_{2\rho} \\ \vdots \\ g_{N_c\rho} \end{bmatrix}, \\ & h_{i,j\rho} = [P]_{\rho(i-1)n_u, \rho+(j-1)n_u}, \\ & g_{i\rho} = [C]_{(i-1)n_u+\rho} + 1/2 \sum_{j=1}^{N_c} \sum_{\lambda=1, \lambda \neq \rho}^{n_u} \Delta u_\lambda[j-1] \\ & \quad * ([P]_{\rho+(i-1)n_u, (j-1)n_u+\lambda} + [P]_{(j-1)n_u+\lambda, \rho+(i-1)n_u}), \\ & \quad i, j \in \{1, \dots, N_c\}. \end{aligned}$$

A QP solver is developed based on the following active set method algorithm [27], and it is hard coded in the distributed IIoT-based smart thermostats that we design and develop for the practical implementation. The active set method algorithm

is concerned with the solution of the following constrained quadratic convex optimization problem:

$$\min_u J(u), \quad J(u) = \frac{1}{2} u^{tr} Q u + q^{tr} u, \quad Q > 0$$

subject to $Au = a$ and $Bu \leq b$.

Strategy [27]:

- Start from an arbitrary but feasible point u^0
- Find the next iterate by setting $u^{t+1} = u^t + \alpha^t d^t$.

Note that the non-negative scalar α^t is the step length and the vector d^t is the search direction. Now, the questions are how to determine the search direction d^t and the step length α^t so that $u^t + \alpha^t d^t$ is feasible.

d^t is chosen using the following algorithm:

Algorithm for finding d^t :

- At the current iterate u^t determine the index set of active inequality constraints: $\mathcal{A}^k = \{j | b_j^{tr} u^t - b_j = 0, j = 1, 2, \dots, m_2\}$, where b_j is a column of the matrix B that corresponds to the j th active inequality constraint.
- Solve the direction finding problem using KKT method [27] or the Newton's method: $\min_d (\frac{1}{2} d^{tr} Q d + g^{tr} d)$, $g = Qu^t + q$ subject to $Ad = 0$ and $\tilde{B}d = 0$, where \tilde{B} is a matrix with b_{j_s} as their columns.

Having that, the optimal solution u^* is obtained as follows:

- Start from an arbitrary but feasible vector u^0
- Identify the active index set \mathcal{A}^0
- Find d^0
If $d^t = 0$, stop. u^t is the optimal solution
If $d^t \neq 0$, update α^t so that $u^t + \alpha^t d^t$ is feasible and then update $u^{t+1} = u^t + \alpha^t d^t$ and go back and find the active index set \mathcal{A}^{t+1} and repeat the above procedure until $d^t = 0$.

Based on the above algorithm we have developed a general QP solver and hard coded it in the smart thermostats for solving the following quadratic convex constrained optimization problem:

$$\min_{\Delta U_\rho} \left(\frac{1}{2} \Delta U_\rho^{tr} H_\rho \Delta U_\rho + G_\rho^{tr} \Delta U_\rho \right), \quad H_\rho > 0$$

subject to $\Delta U_{min} \leq \Delta U_\rho \leq \Delta U_{max}$, where $\Delta U_{min} = [\Delta u_{min}^{tr} \ \dots \ \Delta u_{min}^{tr}]^{tr}$ and $\Delta U_{max} = [\Delta u_{max}^{tr} \ \dots \ \Delta u_{max}^{tr}]^{tr}$.

IV. THE STRUCTURE OF THE CYBER-PHYSICAL SYSTEM FOR THE OPTIMAL HEATING-COOLING OF BUILDING

This section presents the structure of the proposed cyber-physical system for the optimal heating-cooling of building. In Fig. 2, the network structure of the proposed system is shown. In this structure, each room is equipped with a smart IIoT-based thermostat that is described with details in Section VI. Note that each room is equipped with at least one fan-coil unit. In winter time fan-coil unit is supplied with hot water produced by centralized boiler and in summer season it is supplied with cold water produced by chiller.

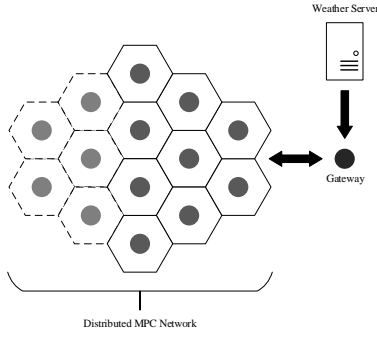


Fig. 2: The structure of the proposed CPS for the optimal heating-cooling of building

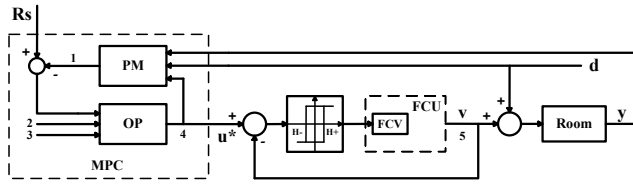


Fig. 3: The block diagram of the proposed control strategy in each room. 1: Predicted Output, 2: Constraints, 3: Cost Functions, 4: Predicted Input, 5: Fan-Coil Air Temperature, PM: Plant Model, OP: Optimizer

The output temperature of the fan-coil unit is controlled by a fan and a electric valve that controls the input flow rate of hot/cold water to fan-coil unit. Sub-MPC problems are embedded in smart distributed thermostats forming a distributed MPC network. Each smart thermostat solves its sub-MPC problem in collaboration and communication with other smart thermostats to determine the proper set-point for its fan-coil units output temperature. In the proposed structure there is a gateway in the network that connects the distributed MPC network to a computer server connected to the Internet for monitoring and intervention by high level supervisor. This gateway receives the weather forecast data from the server and broadcasts it to all smart thermostats for feed-forwarding.

In Fig. 3, the proposed control structure for each room is shown. Using the proposed DMPC method, the optimal HVAC set-points that regulate rooms' temperature around the desired set-point (R_s) is computed by the distributed MPC network with the period of LT_s seconds, where L is the re-sampling period and T_s is the sample rate that we sample the rooms temperature. Note that in the dynamic model (1) the time period between to successive time instants, k and $k + 1$ is LT_s seconds. To apply the computed HVAC set-points generated by the proposed DMPC method to the fan-coil units, an hysteresis control structure, as shown in Fig. 3, is used. This method enables us to equip fan-coil units to On-Off valves for HVAC temperature regulation, which are cost effective. The simulation results and the practical implementation results given in Sections V and VI illustrate that using this set-up, the satisfactory performance is achieved.

In order to guarantee the feasibility of distributed optimizers u_{min} and u_{max} in the problem formulation of Section III should be dynamic depending on the season. In HVAC

systems, there are two HVAC modes: heating (winter season) and cooling (summer season). If the HVAC system works in heating mode, the minimum temperature of the fan-coil unit occurred when the valve and/or fan of the fan-coil unit is off; and hence, the minimum fan-coil unit temperature is equal to the room temperature at that time. Similarly; when the HVAC system works in cooling mode (summer season), the maximum temperature of the fan-coil unit occurred when the valve and/or fan of the fan-coil unit is off; and hence, the maximum fan-coil unit temperature is equal to the room temperature at that time. Thus; the inequality constraints for the optimization problem formulated in Section III should be re-formulated as follows to comply with the feasibility of the problem:

HVAC Heating Mode:

$$y_\rho - u_\rho[k_i + q - 1] \leq \Delta u_\rho[k_i + q],$$

$$\Delta u_\rho[k_i + q] \leq u_{max} - u_\rho[k_i + q - 1].$$

HVAC Cooling Mode:

$$u_{min} - u_\rho[k_i + q - 1] \leq \Delta u_\rho[k_i + q],$$

$$\Delta u_\rho[k_i + q] \leq y_\rho - u_\rho[k_i + q - 1].$$

V. SIMULATION RESULTS

In this section we apply the proposed cyber-physical system equipped with the proposed EI-MPC to a 6-story building with 40 rooms to regulate its rooms temperature. We compare the proposed EI-MPC performance with the performances of the available DMPC (e.g., proposed in [7], [4]) for the temperature regulation of this building, and also the performance of the traditional hysteresis - based method [3]. We use the Design Builder Software [28] to model the thermal behaviour of this 6-story building with 40 rooms, as shown in Fig. 4. Using this software, the thermal model of this building has the following linear state space representation:

$$x_m[k + 1] = A_m x_m[k] + B_m u[k] + E_m d[k]$$

$$y[k] = C_m x_m[k] \quad (8)$$

where here x_m is the state vector of the system, v is the decision vector of the system (the temperature of HVAC units), y is the sensor measurements (rooms temperature) and d is the measurable disturbance vector, $d[k] = [T_a[k] T_c[k] T_f[k]]^{tr}$, where T_a is the measurable outside temperature, T_c is the unknown corridor floors temperature, and T_f is the unknown first floor ground temperature. We extract the matrices coefficients A_m , B_m , C_m and E_m from the Design Builder software.

Note that the measurable outside temperature T_a is feed-forwarded to design the controller and T_c and T_f does not considered in the design of controller and that are treated as unknown disturbances. For simulation it is assumed that $n_o = 40$, $n_i = 40$, $n_s = 40$, $T_s = 60$ seconds and $L = 5$. The authorized static bounds for the decision variables are $u_{min} = 16$ Centigrade, $u_{max} = 50$ Centigrade, $\Delta u_{max} = +4$ Centigrade and $\Delta u_{min} = -4$ Centigrade. The control horizon should be selected based on the transient response of the

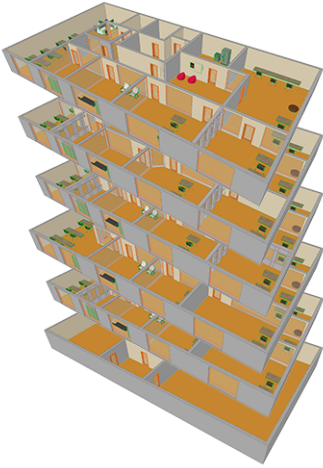


Fig. 4: A view of the 6-story building used for simulation

thermal dynamic of the building; and we choose it to be $N_p = N_c = 10$. Throughout, we set $R = 0.05I$ and $Q = I$ and the number of iterations for distributed optimization is set to be 100. To simulate the fan-coil unit and On-Off valve operation, the first order response model is used for fan-coil air temperature modelling and the first order time constant is chosen to be $\tau = 2min$. In simulation, the outside temperature varies and throughout it is assumed that the speed of the fan-coil units is set for high and the fan-coil units temperature is controlled by On-Off valves .

In Figs. (5, 6, 7,8), it is assumed that the fan-coil units are in the heating mode (winter session) and the outside temperature varies between $T_a = [12, 18]$ Centigrade and corridor floors and ground floor temperatures are assumed to be $T_c = 25$ Centigrade and $T_f = 15$ Centigrade, respectively. The room initial temperature is assumed to be 18 Centigrade.

Having that, Fig. 5 illustrates the system's response for the temperature regulation around set-points 23 Centigrade and 26 Centigrade when the control variables are generated from the centralized EI-MPC method. From this figure it is clear that the temperature of each room reaches to the desired temperature with minor fluctuations around it indicating zero steady - state error; and the maximum temperature of the fan-coil units reaches to 36. Fig. 6 illustrates the system's response when the control variables are generated from the standard DMPC (proposed in [7], [4]). This figure illustrates a large steady state error. Fig. 7 illustrates the response when the control variables are generated from the proposed distributed EI-MPC with the number of iterations equal to 100 that distributes the computational load of the centralized EI-MPC to distributed thermostats. This figure illustrates a response similar to centralized EI-MPC. Fig. 8 illustrates the response of the traditional hysteresis-based method. In this figure different colors are used for different rooms. Top figure illustrates that there are high fluctuation (± 1 Centigrade) around the desired set points of 23 Centigrade and 26 Centigrade. Bottom figure illustrates that the temperatures of the fan-coil units are frequently changing between 24 Centigrade and 50 Centigrade. From these figures, it follows that the proposed EI-MPC method

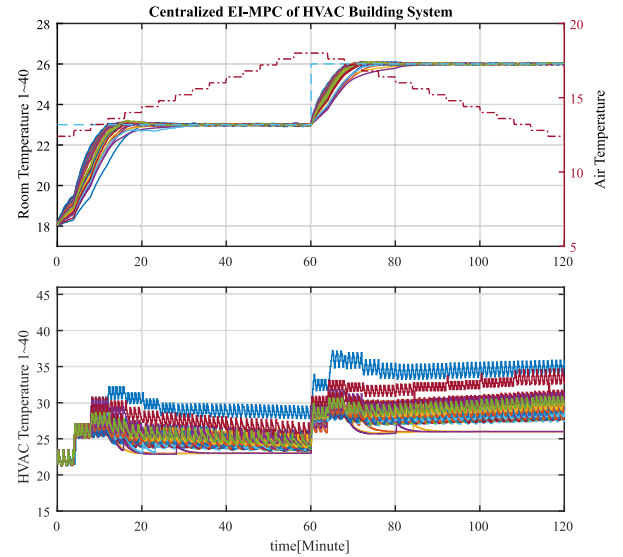


Fig. 5: Temperature regulation response of the case study building for the heating mode when the centralized EI-MPC is used. Different colors are used for different rooms. Top figure illustrates that the temperature of each room reaches to the desired temperature. Bottom figure illustrates control efforts.

results in a better performance compared with the standard DMPC method previously proposed in [7] and [4] in terms of temperature regulation. It results in minor fluctuations around desired temperature indicating zero steady-state error; while the available results in the literature result in very large steady-state error. It also results in limited start-up fan-coil units temperature that results in the start-up energy consumption optimization, which is beneficial in winter time for temperature regulation. From the simulation results it also follows that the distributed EI-MPC method results in a performance similar to the performance of the centralized EI-MPC; but with much less computational complexity. This is especially beneficial for large-scale buildings, where the computational complexity associated with the centralized EI-MPC is considerable high. Note that as shown in [2], the computational complexity of the centralized method is of the order of $O(n^5)$. In contrast, the computational complexity associated with the distributed method is of the order of $O(n)$. Hence, the distributed EI-MPC is especially useful in large-scale buildings with many rooms. From Fig. 8, it follows that the performance of the traditional hysteresis-based method is poor in terms of the response and the control efforts. Specifically, the temperature of the centralized boiler should be set at least 14 Centigrade higher than that of the proposed MPC based methods. In other words, using the proposed EI-MPC methods, we can reach the same desired room temperature with zero steady-state error and significantly lower centralized boiler temperature. This means saving lots of energy for heating building. This result is also verified in the practical implementation section.

In Figs. (9, 10, 11, 12), it is assumed that the fan-coil units are in the cooling mode (summer session) and the outside temperature varies between $T_a = [28, 34]$ Centigrade and corridor floors and ground floor temperatures are assumed to be $T_c = 25$ Centigrade and $T_f = 28$ Centigrade,

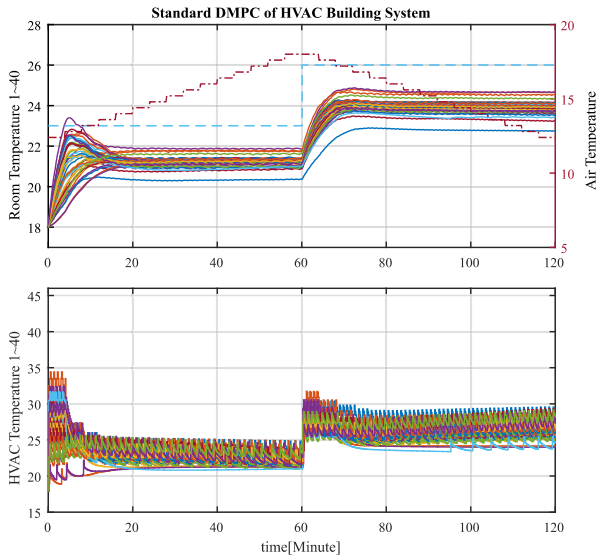


Fig. 6: Temperature regulation response of the case study building for the heating mode when the distributed standard MPC of [7] and [4] is used. Top figure illustrates large steady state error in temperature regulation around the desired set points of 23 Centigrade and 26 Centigrade.

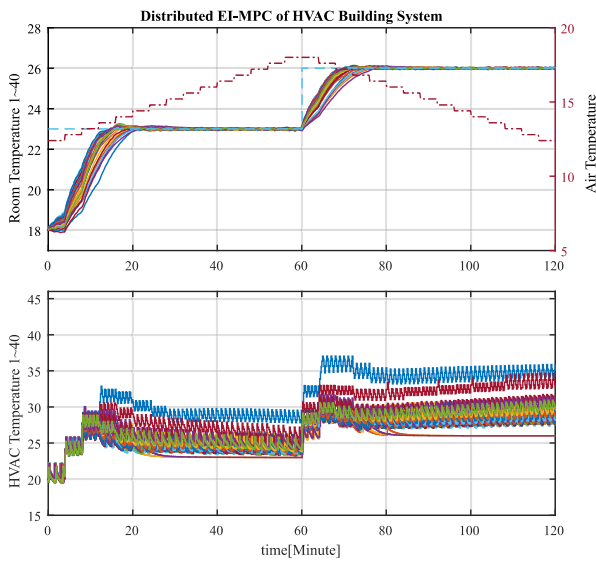


Fig. 7: Temperature regulation response of the case study building for the heating mode when the proposed distributed EI-MPC is used. Top figure illustrates that the temperature of each room reaches to the desired temperature. Bottom figure illustrates similar control efforts as the centralized EI-MPC.

respectively. The room initial temperature is assumed to be 30 Centigrade. Fig. 9 illustrates the response of the system for the temperature regulation around set-points 26 Centigrade and 23 Centigrade when the control variables are generated from the centralized EI-MPC method. This figure illustrates that each room reaches to the desired temperature. Fig. 10 illustrates the response when the control variables are generated from the distributed standard MPC method proposed in [7], [4]. This figure illustrates large steady state error. Fig. 11 illustrates the response when the control variables are generated from the proposed distributed EI-MPC with the number of iterations equal to 100 that distributes the

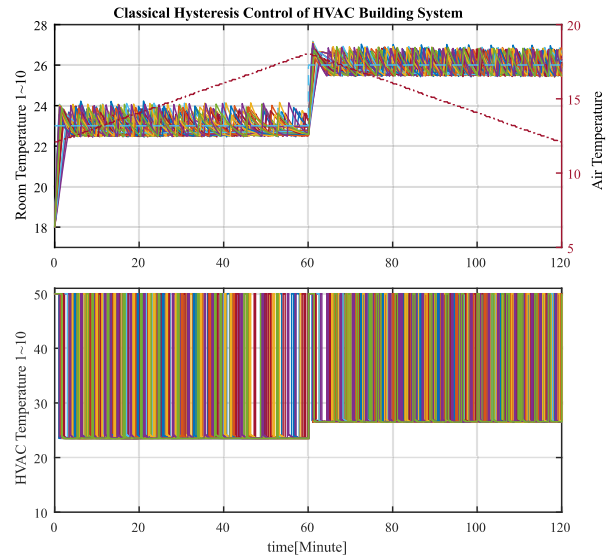


Fig. 8: Temperature regulation response of the case study building for the heating mode when the traditional hysteresis-based method is used. Different colors are used for different rooms. Top figure illustrates that there are high fluctuation (± 1 Centigrade) around the desired set points of 23 Centigrade and 26 Centigrade. Bottom figure illustrates that the temperature of the fan-coil units are frequently changing between 24 Centigrade and 50 Centigrade.

computation load of the centralized EI-MPC to distributed thermostats. This figure illustrates a response similar to centralized EI-MPC. Fig. 12 illustrates the response of the traditional hysteresis-based method. Top figure illustrates that there are high fluctuation (± 1 Centigrade) around the desired set points of 26 Centigrade and 23 Centigrade. Bottom figure illustrates that the temperatures of the fan-coil units are frequently changing between 25 Centigrade and 12 Centigrade. From these figures, it follows that the proposed EI-MPC method also results in a better performance in summer mode compared with the performances of the standard MPC method previously proposed in [7] and [4] and the traditional hysteresis-based method.

In Fig. 13, the effects of using outside (air) temperature feed forward mechanism in rooms temperature regulation is shown. As it is clear from this simulation, the air temperature feed forward mechanism; and in particular, air temperature forecast feed forwarding have significant effect in improving the transient response of the rooms temperature regulation.

VI. THE PRACTICAL IMPLEMENTATION RESULTS

To evaluate the performance of the proposed distributed MPC method for the optimal heating-cooling of buildings, we design and develop the smart thermostat of Fig. 14 and a gateway. For the practical implementation we use two smart thermostats. Each smart thermostat includes an on-board temperature and humidity sensor for measuring the room temperature and humidity. It also provides light and motion detection sensors, two one-wire temperature sensors for measuring the fan coil unit temperature, two digital outputs for activating two electric valves, two electric relays for activating the fan-coil unit's fan, and an ESP32 IIoT module for data exchange

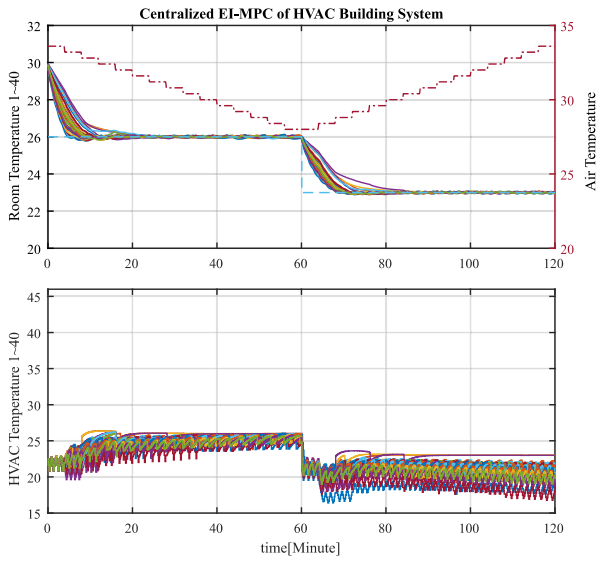


Fig. 9: Temperature regulation response of the case study building for the cooling mode when the centralized EI-MPC is used. Different colors are used for different rooms. Top figure illustrates that the temperature of each room reaches to the desired temperature. Bottom figure illustrates control efforts for such a good temperature regulation.

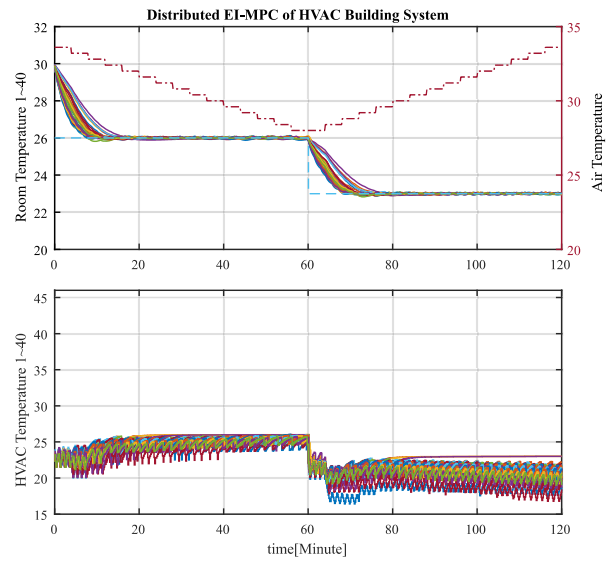


Fig. 11: Temperature regulation response of the case study building for the cooling mode when the proposed distributed EI-MPC is used. Top figure illustrates that the temperature of each room reaches to the desired temperature. Bottom figure illustrates similar control efforts as the centralized EI-MPC.

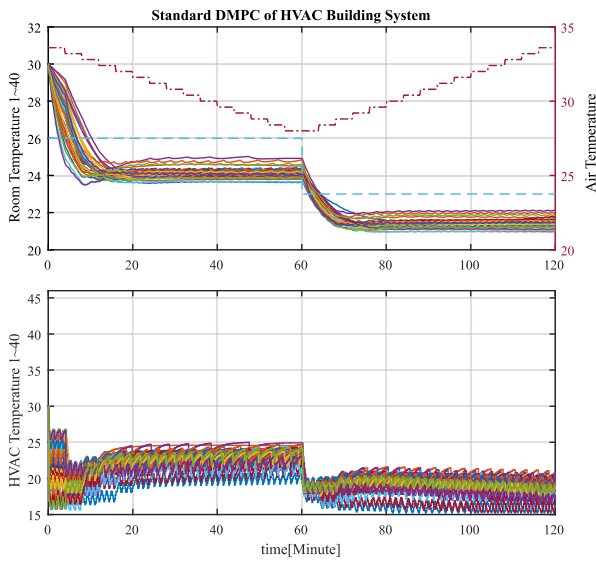


Fig. 10: Temperature regulation response of the case study building for the cooling mode when the distributed standard MPC of [7] and [4] is used. Top figure illustrates large steady state error around the desired set points of 26 Centigrade and 23 Centigrade.

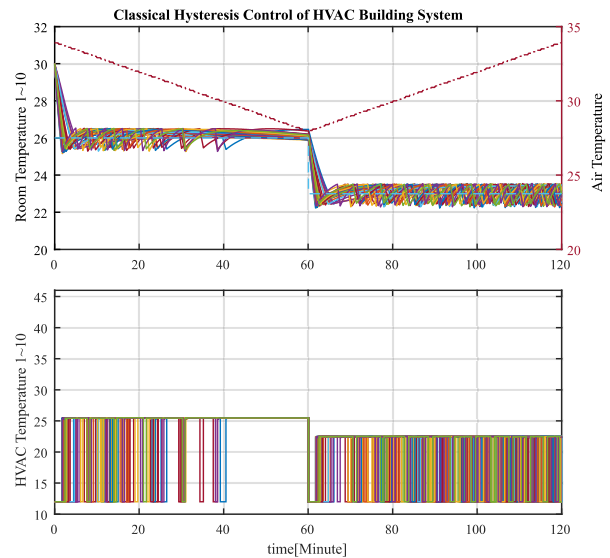


Fig. 12: Temperature regulation response of the case study building for the cooling mode when the traditional hysteresis-based method is used. Top figure illustrates that there are high fluctuation (± 1 Centigrade) around the desired set points of 26 Centigrade and 23 Centigrade. Bottom figure illustrates that the temperature of the fan-coil units are frequently changing between 25 Centigrade and 12 Centigrade.

between the smart thermostats and gateway. Note that each smart thermostat can monitor and control at maximum two fan coil units simultaneously. The ESP32 module consists of two cores. We use one for handling data exchange and the other one for centralized or distributed computation.

Using this set-up, we aim to regulate the temperature of one of the rooms of the 6-story building used in Section V for simulation. This room is equipped with two fan-coil units as shown in Fig. 15. For the temperature regulation of this room we need a plant model for each room. This model is obtained by the Design Builder software used for simulation study. This is a commercial widely used software

for thermal modelling of buildings. This software uses the building plan and builds thermal model. Obviously, there is mis-match between the model and the thermal behaviour of the room. But as we have shown in [4] using feedback this mis-match is compensated. Using this set-up we aim to compare the performances of the centralized EI-MPC, the distributed standard MPC proposed in [7] and [4], the proposed distributed EI-MPC and the traditional hysteresis-based control method using the available thermostat of the room. In this way, we can verify the simulation results presented in Section V for

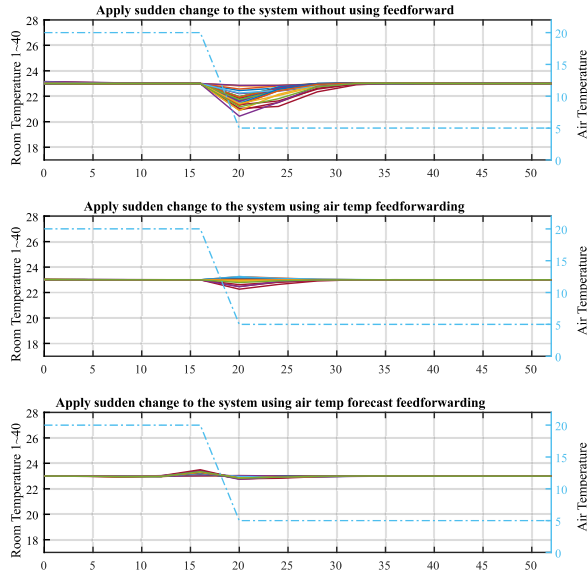


Fig. 13: The effects of not using/using feed-forward mechanism for the rooms temperature regulation. Top figure: without outside (air) temperature feed-forward mechanism. Middle figure: with air temperature feed forwarding. Bottom figure: with air temperature forecast feed forwarding

the large-scale building of Section V in a small-scale. The thermal dynamic of the room is as follows:

$$\begin{aligned} x_m[k+1] &= A_m x_m[k] + B_m u[k] + E_m d[k] \\ y[k] &= C_m x_m[k] \end{aligned} \quad (9)$$

where $A_m = 0.7808$, $B_m = [0.0523 \ 0.0523]$, $E_m = [0.0507 \ 0.0639]$, $C_m = 1$ and $d[k] = \begin{bmatrix} T_a \\ T_o \end{bmatrix}$. T_o is the temperature of the other rooms, which is unknown and considered as disturbance. Throughout experiments, fan speed is set for the high speed; the decision variable is the fan-coil unit temperature, which is controlled by the smart thermostat via controlling the on/off duty cycle of the electric valve installed on the water path of the fan-coil unit. We use two smart thermostats to implement the distributed method, each responsible for controlling one fan-coil unit. For the other cases, we use only one smart thermostat that controls both fan-coil units. Each method is implemented for 24 hours from 12 PM to 11:59 AM in the next day. The smart thermostats are set for the heating mode (as we were in the winter session during experiments), the temperature of the centralized boiler of the building is set to be 60 Centigrade and $u_{min} = T_{room}$ and $u_{max} = 50$ Centigrade, respectively. The room desired temperature (set-point) is set for 25 and $\Delta u_{max} = 4$ Centigrade and $\Delta u_{min} = -4$ Centigrade. From 8 AM (in the morning) to 16 (in the afternoon), the room is occupied by 2 or 3 students. They frequently open windows during these hours for fresh air. This can be considered as disturbance to the system. Despite this disturbance, it is shown here that a satisfactory temperature regulation around the desired set point is achieved; while there is mis-match between the model and the actual thermal behaviour of the room. This is due to the existence of feedback control for the temperature regulation. For the MPC-based methods, the configuration coefficients are



Fig. 14: The developed smart thermostat



Fig. 15: A view of the room equipped with smart thermostats

set to be $R = 0.05$ and $Q = 1$. Then, MPC Strategy updates the desired temperature of the fan-coil unit every 5 minutes. Subsequently, using a closed loop control strategy as shown in Fig. 3 by measuring the temperature of the fan-coil unit each minute, the smart thermostat correctly open or close the electric valve of the fan-coil unit to make sure that the fan-coil unit temperature reaches to the desired temperature obtained by the MPC strategy.

Having that, Figs. (16, 17, 18, 19) illustrate practical implementation results. Fig. 16 illustrates the results of the room temperature regulation around the desired set-point of 25 Centigrade using the centralized EI-MPC. Also, Fig. 17, Fig. 18, and Fig. 19 illustrate the results of the room temperature regulation around the desired set-point (i.e., 25 Centigrade) using the proposed distributed EI-MPC, the distributed standard MPC proposed in [7] and [4] and the traditional hysteresis-based control using the available thermostat of the room. In Table I, we compare these control strategies with each other. As it is clear from this table and figures, all methods could eventually regulate the room temperature around the desired set-point of 25 Centigrade; but by looking at the average room temperature and the variation of the room temperature around the desired set-point of 25 Centigrade; it is clear that the proposed distributed EI-MPC and the centralized EI-MPC have much better performance compared with other methods, i.e., the standard MPC method proposed in [7] and [4] and the traditional hysteresis-based method.

Temperature[°C]	Control Method			
	Centralized EI-MPC	Distributed EI-MPC	Standard MPC	Hysteresis Control
Room (avg)	25.01	25.02	25.71	25.42
Room (Min)	23	23.5	20.25	24.25
Room (Max)	27	26.25	27.25	28.25
Room (var)	0.34	0.19	2.16	0.9825
Mean Fan-coil (avg)	28.3	28.71	28.46	28.16
Mean Fan-coil (Min)	23.37	24.4	26.59	23.09
Mean Fan-coil (Max)	36.71	37.28	30.68	39.25
Mean Fan-coil (var)	12.04	9.23	0.69	20.61
Air (avg)	13.36	13.27	12.24	12.79
Air (Min)	10	9	8	8
Air (Max)	16	18	17	18
Air (var)	2.40	11.64	9.85	9.25

TABLE I: Performance comparison between different methods. Mean Fan-coil temperature means the average temperatures of two fan-coil units.

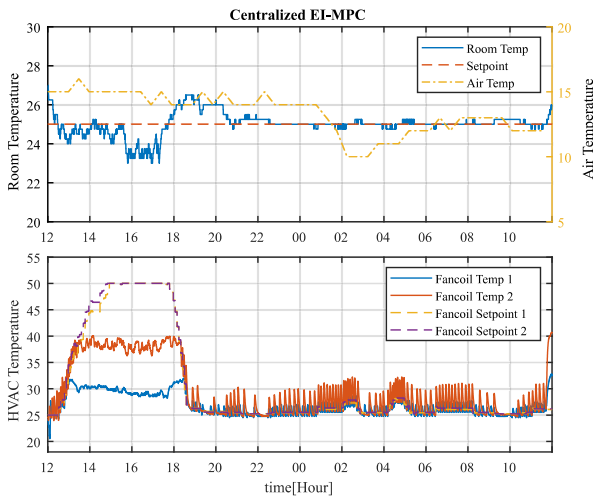


Fig. 16: Room temperature regulation response when the centralized EI-MPC is used

Specifically, the proposed method results in zero steady-state error; while the traditional method and the available method in the literature result in a large and unacceptable steady-state error. This result is consistent with the simulation results and it verifies the simulation results for the 6-story building in a small-scale. In particular, Fig. 17 illustrates that for most of the time, the HVAC temperatures of the two fan-coil units of the room when the distributed EI-MPC is used, is around 25 Centigrade; except for 3 hours that reaches to 40 Centigrade. In comparison, this time is almost half of the times that the HVAC temperature of the classical hysteresis based method (i.e., Fig. 19) reaches to 40 Centigrade. Hence; if the centralized boiler is only responsible for these two fan-coil units, the required time that the centralized boiler needs to be turned on for the proposed EI-MPC method is almost half of the time for the classical method. This means energy saving.

VII. CONCLUSION AND FUTURE RESEARCH DIRECTION

This paper proposed a novel cyber-physical system for the optimal heating-cooling of buildings. For the future, it is interesting to equip the whole rooms of this 6-story building with smart IIoT-based thermostats. This research direction is currently under way in our research team by equipping the 6-story building with the commercial version of the smart thermostat developed in this paper, as shown in Fig. 20. In this way, we may even have better results; because for the case of one room, the temperature of surrounding rooms is considered

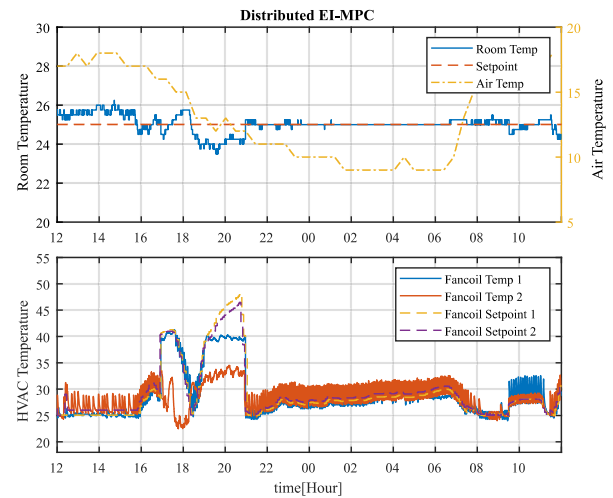


Fig. 17: Room temperature regulation response when the distributed EI-MPC is used

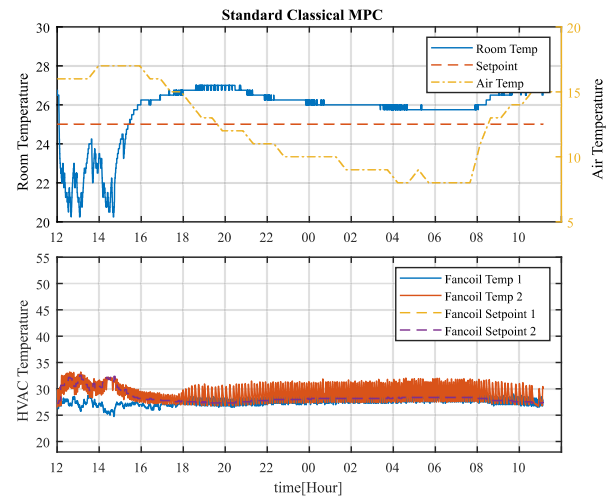


Fig. 18: Room temperature regulation response when the distributed MPC proposed in [7], [4] is used

as disturbance; while for the other case, the controllers of surrounding rooms collaborate with the controller of the room of Fig. 15 for the temperature regulation.

REFERENCES

- [1] Shaoyuan Li, Yi Zheng, Distributed model predictive control for plant-wide systems. Wiley, 2015.
- [2] Farhadi, A., Dower, P. M. and Cantoni, M. Computation time analysis of a centralized and distributed optimization algorithms applied to automated irrigation networks. in Proceedings of the 2013 Australian Control Conference (AUCC), November 4-5, 2013, Perth, Australia, pp. 263-269
- [3] Ross Montgomery P.E. and Robert McDowall P. Fundamentals of HVAC Control Systems. Elsevier Science, 2008.
- [4] Karbasi, A. and Farhadi, A. A cyber-physical system for building automation and control system based on a distributed MPC with an efficient method for communication. European Journal of Control, vol. 61, pp. 151 - 170, 2021.
- [5] Moros, P. D., Bourdais, R., Dumur, D. and Buisson, J. Building temperature regulation using a distributed model predictive control. Energy and Buildings, vol. 42, no. 9, pp. 1445 - 1452, 2010.
- [6] Barata, F. A., Igreja, J. M. and Neves-Silva, R. Distributed MPC for thermal comfort and load allocation with energy auction. International Journal of Renewable Energy Research (IJRER), vol. 4, no. 2, pp. 371 - 383, 2014

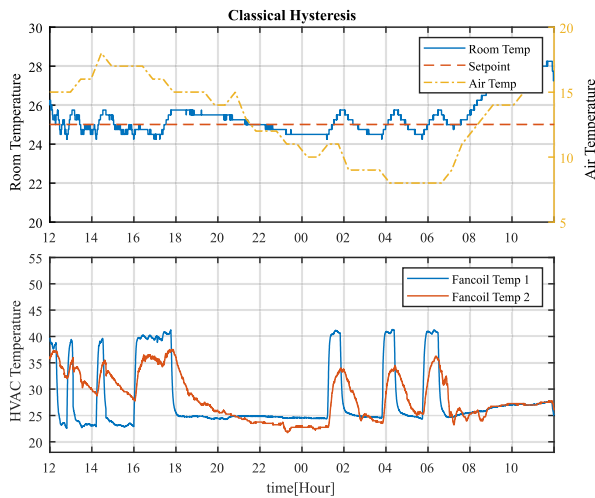


Fig. 19: Room temperature regulation response when the available hysteresis-based control method is used



Fig. 20: A smart IIoT-based thermostat

[7] Farhadi A. and Khodabandehlou, A., Distributed model predictive control with hierarchical architecture for communication: application in automated irrigation channels. *International Journal of Control*, 89(8), pp. 1725 - 1741, August 2016.

[8] Ma Y., Anderson G. and Borrelli F. A distributed predictive approach to building temperature regulation. *American Control Conference (ACC)*, pp. 2089 - 2094, 2011.

[9] Ma Y., Kelman A., Daly A. and Borrelli F. Predictive control for energy efficient buildings with thermal storage. *IEEE Control System Magazine*, 32(1), 2012.

[10] Siroky J., Oldewurtel F. and Cigler J. and Privara S. Experimental analysis of model predictive control for an energy efficient building heating system. *Applied Energy*, 88(9), pp. 3079 - 3087, 2011.

[11] Ma J. Qin S. J. and Salsbury T. Model predictive control of building energy systems with balanced model reduction. *American Control Conference (ACC)*, pp. 3681 - 3686, 2012.

[12] Hou X. Xiao Y., Cai J., Hu J. and Braun J. E. A distributed model predictive control approach for optimal coordination of multiple thermal zones in a large open space. *The 4th International High Performance Buildings Conference*, 2016.

[13] Barata, F. A., Igreja J. M. and Neves-Silva R. Distributed MPC for thermal comfort and load allocation with energy auction. *International Journal of Renewable Energy Research (IJRER)*, 4(2), pp. 371 - 383, 2014.

[14] Al-Azba M., Cen Z., Remond Y. and Ahzi S. An optimal air-conditioner on-off control scheme under extremely hot weather conditions. *Energies*, 1021, 2020. <https://doi.org/10.3390/en13051021>.

[15] Serale G., Fiorentini M., Capozzoli A., Bernardini D. and Bemporad A. Model predictive control (MPC) for enhancing building and HVAC system energy efficiency: problem formulation, applications and opportunities. *Energies*, 631 (11), pp. 1 - 35, 2018. <https://doi.org/10.3390/en11030631>.

[16] Carli R, Cavone G., Ben Othman S., Dotoli M. IoT Based Architecture for Model Predictive Control of HVAC Systems in Smart Buildings. *Sensors*. 20(3), pp. 781 - 799, 2020.

[17] Jaewon J, Panagiota K. A model predictive control strategy to optimize

the performance of radiant floor heating and cooling systems in office buildings. *Applied Energy*. pp. 65 - 77, 2019.

[18] Yudong X., Ming Z., Aipeng J., Jian W., Xiaoxia B., Shiming D.. Model predictive control of indoor thermal environment conditioned by a direct expansion air conditioning system. *Building Simulation*. 16, pp. 357 - 378, 2023.

[19] Ping J, Chenxi J, Shi L, Wenxue X, Yu Q. Model predictive control of heating process with weather forecast compensation. *IEEE Symposium series on computational intelligence (SSCI)*. December 6-9, 2019.

[20] Yaïci W, Entchev E, Longo M. Internet of Things (IoT)-Based System for Smart Home Heating and Cooling Control. *2022 IEEE International Conference on Environment and Electrical Engineering and 2022 IEEE Industrial and Commercial Power Systems Europe*.

[21] Barbiero M, Rossi A, Schenato L. LQR temperature control in smart building via real-time weather forecasting. *29th Mediterranean Conference on Control and Automation (MED)*, 2021.

[22] Mazar M, Rezaeizadeh A. Adaptive model predictive climate control of multi-unit buildings using weather forecast data. *Journal of Building Engineering*. Volume 32, November 2020.

[23] Chen Q, Li N, Feng W. Model predictive control optimization for rapid response and energy efficiency based on the state-space model of a radiant floor heating system. *Energy and Buildings*, Volume 238, 2021.

[24] Kardos T, Kutasi D N, György, K. Control strategies for HVAC systems. *IEEE Joint 19th International Symposium on Computational Intelligence and Informatics and 7th IEEE International Conference on Recent Achievements in Mechatronics, Automation, Computer Sciences and Robotics*, Szeged, Hungary, November 14-16, 2019.

[25] Anuntasethakul C, Banjerdpongchai D. Design of Supervisory Model Predictive Control for Building HVAC System with Consideration of Peak-Load Shaving and Thermal Comfort. *IEEE Access*. March 2021.

[26] Yao Y, Shekhar D. K. State of the art review on model predictive control (MPC) in Heating Ventilation and Air-conditioning (HVAC) field. *Building and Environment*, 2021.

[27] Potschka A., Kirches C., Bock H. G. and Shloder J. P. Reliable solution of convex quadratic programs with parametric active set methods. *Optimization Online*, 2011.

[28] Builder D. Design builder software ltd, Recuperado de: <https://www.designbuilder.co.uk>, 2009.

BIOGRAPHY SECTION



Mahdiyar Barzegar received the M.Sc. degree from the Department of Electrical Engineering with concentrations on Digital Electronics Systems, Sharif University of Technology, Tehran, Iran, in 2023. His current research interests are concerned with embedded systems, cyber-physical systems, distributed control systems, and fuzzy control systems. Email: mahdiyar.barzegar@sharif.edu



Alireza Farhadi is Associate Professor in the Department of Electrical Engineering, Sharif University of Technology, Tehran, Iran. His research interests are concerned with automation and control, IIoT, CPS and their applications in HVAC systems, water management, etc. Email: afarhadi@sharif.edu